

Supporting Information

Cucurbit[7]uril promoted Fenton oxidation through modulating the redox property of catalyst

Bohan Tang¹, Jiantao Zhao¹, Yang Jiao, Jiang-Fei Xu and Xi Zhang*

Key Laboratory of Organic Optoelectronics & Molecular Engineering, Department of Chemistry, Tsinghua University, Beijing 100084 (China)

E-mail: xi@mail.tsinghua.edu.cn

1. General instrumentation and methods.

The NMR spectra were obtained using a JOEL JNM-ECA400 apparatus. ESI-mass spectroscopy was carried out on a LTQ LC/MS apparatus. The UV-Vis spectra were measured using a HITACHI U-3010 spectrophotometer. For all the experiments using UV-Vis spectroscopy, the path length was 10.0 mm. The fluorescence spectra were measured using a HITACHI F-7000 apparatus. The excitation wavelength was 370 nm. Electronic paramagnetic resonance (EPR) measurements were performed on a JEOL JESFA200 apparatus. Isothermal titration calorimetry (ITC) experiments were carried out with a Microcal VP-ITC apparatus in acetic buffer (pH = 4.74) at 298.15 K.

The electrochemical measurements were carried out with the three-electrode system using a CHI-660E electrochemical workstation. Glass carbon disk (0.07 cm²) was served as the working electrode with a Pt wire counter electrode and a saturated calomel electrode (Hg/HgCl₂, KCl saturated) reference electrode. GC electrode was polished with 0.3 and 0.05 μm alumina (Al₂O₃) successively and washed with deionized water before use. NaCl solution was used as supporting electrolyte.

2. Synthesis of (ferrocenylmethyl)ethyltrimethylammonium bromide (FcN)

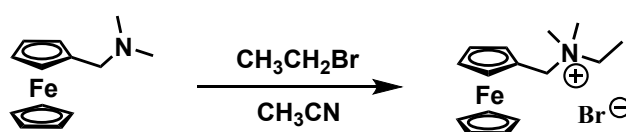


Figure S1. Synthetic route of FcN.

200 mg (182 μ L) N,N-dimethylaminomethylferrocene and 1.0 mL ethyl bromide were added into 10 mL CH_3CN and stirred at 60 $^\circ\text{C}$ overnight. The mixture was then added into 120 mL diethyl ether. The brown precipitate was collected by filtration and washed by diethyl ether for three times.

$^1\text{H-NMR}$ (400 MHz, D_2O , 25 $^\circ\text{C}$): 4.55 (s, 2H), 4.47 (s, 2H), 4.41 (s, 2H), 4.32 (s, 5H), 3.27 (q, $J = 4.8$ Hz, 2H), 2.90 (s, 6H), 1.36 (t, $J = 4.8$ Hz, 3H)

3. The host-guest structure of $\text{FcN/CB}[7]$ and $\text{FcN}^+/\text{CB}[7]$

The host-guest complexation of $\text{FcN/CB}[7]$ was confirmed by $^1\text{H-NMR}$. As shown in Figure S2, the protons on ferrocenyl group shifted upfield indicating that the ferrocenyl group was encapsulated in the cavity of $\text{CB}[7]$.

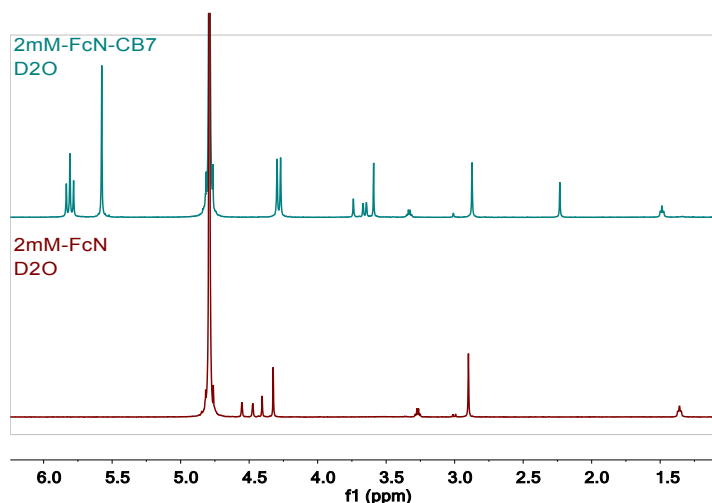


Figure S2. $^1\text{H-NMR}$ spectra of FcN (bottom) and $\text{FcN/CB}[7]$ (up) in D_2O .

FcN^+ was synthesized by FcN with 5 eq. FeCl_3 . After the addition of FeCl_3 , the $^1\text{H-NMR}$ signals on FcN vanished, indicating the generation of paramagnetic FcN^+ (Figure S3).

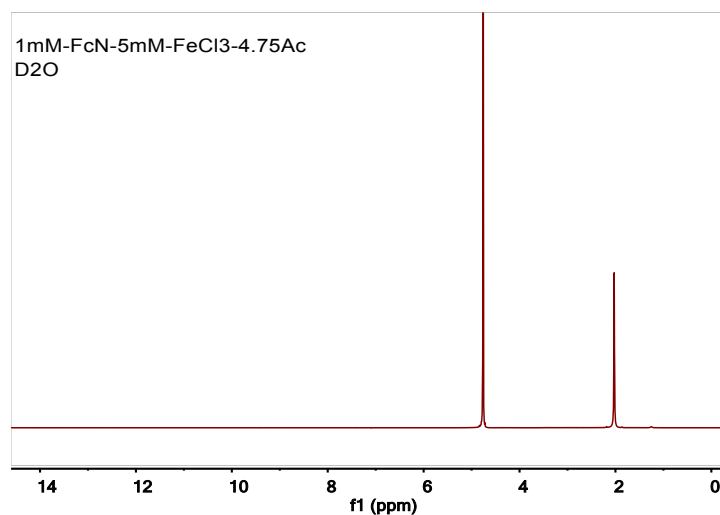


Figure S3. ¹H-NMR spectrum of FcN with 5 eq. FeCl₃ in acetic buffer (pH = 4.75).

According to ITC, Fe³⁺ showed ignorable binding affinity with CB[7]. So the excess Fe³⁺ exhibited little effect on the ITC result of FcN⁺/CB[7] (Figure S4).

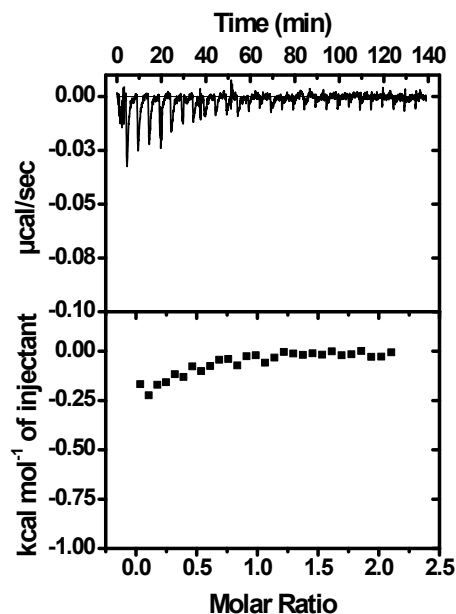


Figure S4. ITC curve of 1 mM FeCl₃ into 0.1 mM CB[7] in acetic buffer (pH = 4.75).

4. Detailed analysis on the kinetics of Fenton oxidation catalyzed by FcN and FcN/CB[7].

According to the basic principle of chemical kinetics, when the initial concentrations of reactants keep constant, the relationship between reaction rate (k) and half-life ($t_{1/2}$) follows:

$$t_{1/2} = \frac{C}{k} \quad (C = \text{constant})$$

where $t_{1/2}$ can be obtained directly from the time-conversion curves.

According to the Arrhenius formula:

$$k = A \exp\left(-\frac{E_a}{RT}\right)$$

where E_a is the apparent activation energy, A is the pre-exponential factor, R is universal gas constant and T is temperature. Thus we can obtain:

$$\frac{C}{t_{1/2}} = A \exp\left(-\frac{E_a}{RT}\right)$$

And then the equation can be further transformed to be:

$$\ln(t_{1/2}) = \frac{E_a}{R} \times \frac{1}{T} + \ln C + \ln A$$

From the data of half-life ($t_{1/2}$) at different temperatures (T), we can obtain the apparent activation energy (E_a) of Fenton oxidation with the linear fitting method, as shown in Figure S4.

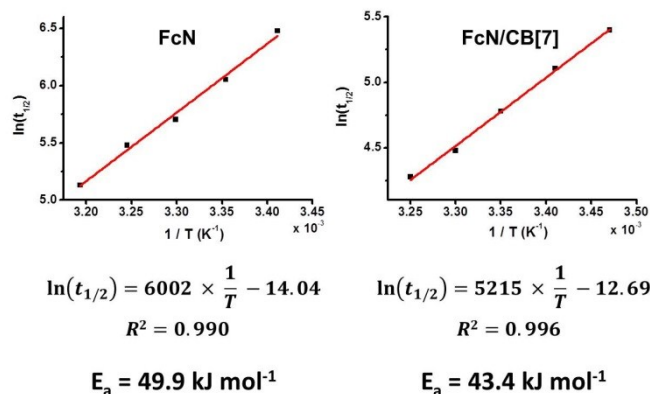


Figure S5. Linear fitting of half-life ($t_{1/2}$) and to reaction temperature (T), to give the apparent activation energy (E_a) of the Fenton oxidation catalyzed by FcN and FcN/CB[7].

5. The structures and oxidation kinetics of Acid Orange 10, Reactive Blue 5, Basic Red 2 and Rhodamine B catalyzed by FcN and FcN/CB[7].

The structures and oxidation kinetics of Acid Orange 10, Reactive Blue 5, Basic Red 2 and Rhodamine B were shown in Figure S5 – S8, respectively. Some dyes were not conducting a one-step oxidation, the conversion-time relationships were replaced by absorption-time relationship. The oxidation processes were monitored by UV-Vis spectroscopy.

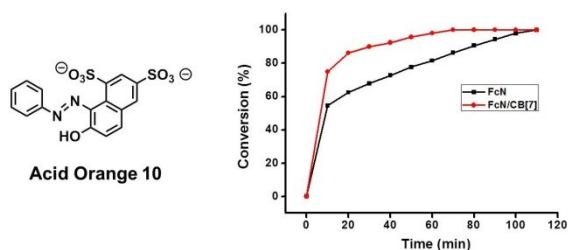


Figure S6. The structures and oxidation kinetics of Acid Orange 10 catalyzed by FcN and FcN/CB[7].

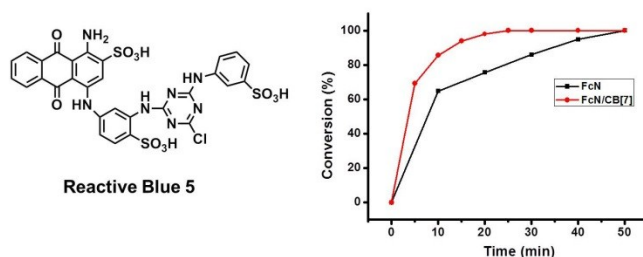


Figure S7. The structures and oxidation kinetics of Reactive Blue 5 catalyzed by FcN and FcN/CB[7].

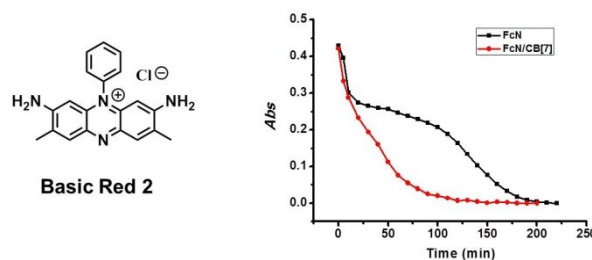


Figure S8. The structures and oxidation kinetics of Basic Red 2 catalyzed by FcN and FcN/CB[7].

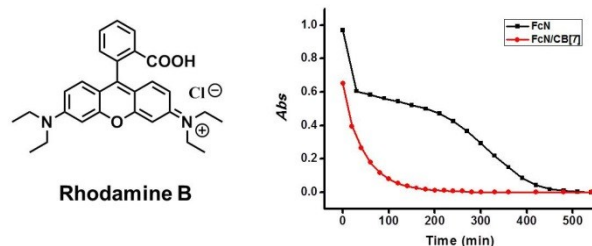


Figure S9. The structures and oxidation kinetics of Rhodamine B catalyzed by FcN and FcN/CB[7].

6. The detailed mechanism of supramolecular modulated Fenton oxidation

The mechanism of Fenton oxidation is listed below¹⁻⁴:

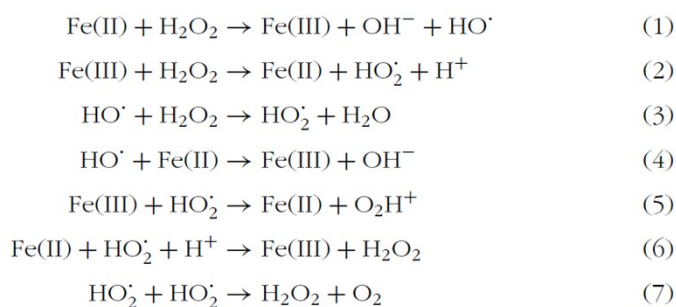


Figure S10. Mechanism of Fenton oxidation

$\bullet\text{OH}$ is generated from the oxidation of Fe(II) to Fe(III). So Fenton oxidation started from Fe(II) can be divided into two phases. First, the quick oxidation of Fe(II), the reaction 1, will lead to an initial rapid degradation phase resulting from a burst of $\bullet\text{OH}$ ⁵. In the second phase, the major species of iron are Fe(III). The generation rate of $\bullet\text{OH}$ is decided by reaction 2, the rate-determining step, because reaction 2 is much slower than reaction 1.

The introduction of CB[7] would promote the reduction of FcN^+ , thus accelerating the reaction 2. Although CB[7] might suppress the oxidation of FcN, the oxidation of FcN/CB[7] was still very fast. Therefore FcN/CB[7] exhibited similar reaction rate in the first phase and higher reaction rate

at the second phase.

According to the mechanism above, the generated $\bullet\text{OH}$ is mostly scavenged by Fe(II) and H_2O_2 (reaction 3, 4). In Fenton oxidation, the concentration of $\bullet\text{OH}$ is always vanishingly small⁶⁻⁷. Therefore, the Fenton oxidation was conducted with excess FcN/CB[7] catalyst. Moreover, because most $\bullet\text{OH}$ was scavenged, the burst of $\bullet\text{OH}$ in the first phase could not oxidize the dyes completely. The complete oxidation time of dyes were almost decided by reaction 2, which is the rate-determining step. And CB[7] made this reduction more favored, thus accelerating the whole Fenton oxidation.

7. The competitive binding of MGCl and CB[7] in Fenton oxidation.

According to ITC, the binding constant of MGCl and CB[7] was too low to have a reliable fitting result (Figure S11). Considering the binding constant of FcN^+ and CB[7] was as high as $2.31 \times 10^6 \text{ M}^{-1}$, the competitive binding of MGCl in Fenton oxidation catalyzed by FcN/CB[7] should be ignored.

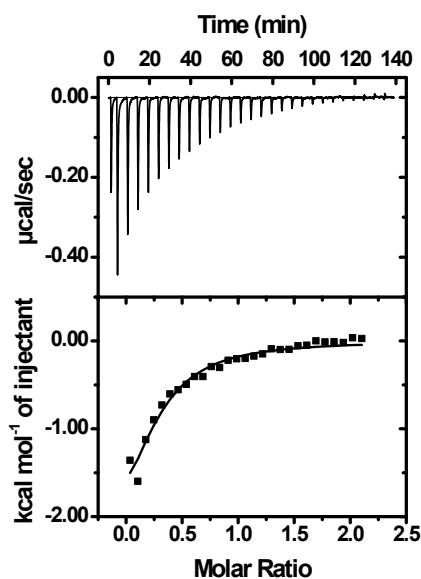


Figure S11. ITC curve of 1 mM CB[7] into 0.1 mM MGCl in acetic buffer ($\text{pH} = 4.75$).

Reference:

1. W. G. Barb, J.H. Baxendale, P. George and K. R. Hargrave, *Nature*, 1949, **163**, 692.
2. W. G. Barb, J.H. Baxendale, P. George and K. R. Hargrave, *Trans. Faraday Soc.*, 1951, **47**, 462.
3. W. G. Barb, J.H. Baxendale, P. George and K. R. Hargrave, *Trans. Faraday Soc.*, 1951, **47**, 591.
4. J. J. Pignatello, E. Oliveros and A. MacKay, *Crit. Rev. Environ. Sci. Technol.*, 2016, **36**, 1.
5. R. Chen and J. J. Pignatello, *Environ. Sci. Technol.*, 1997, **31**, 2399.

6. C. Von Sonntag and H. P. Schuchmann, in *Peroxyl Radicals*, John Wiley and Sons, New York, 1997, 173
7. G. V. Buxton, C. L. Greenstock, W. P. Helman and A. B. Ross, *J. Phys. Chem. Ref. Data*, 1988, **17**, 513.